Advances in Environmental and Life Sciences 5(2) (2024) 1- 20

Contents lists available at Egyptian Knowledge Bank

Advances in Environmental and Life Sciences

journal homepage: https://aels.journals.ekb.eg

Land Use/Land Cover Change Detection and Its Impacts on Carbon Sequestration in the Western Nile Delta, Egypt Using Landsat Data

Abdullah H F Mohamed [a,*], Tarek A Teymuraz [a], Noura E Bakr [b], Khaled A Abutaleb [c,d,e]

[a] *Department of Marine Science-Climate Change Management MSc program, Faculty of Science, Suez Canal University, 45211, Ismailia, Egypt*

[b] *Department of Soils and Water Use, Biological and Agricultural Division, National Research Centre, 11769, Cairo, Egypt*

[c] *National Authority for Remote Sensing and Space Sciences,11769, Cairo, Egypt*

[d] *Agricultural Research Council, Natural Resources and Engineering (ARC-NRE), 0028, Pretoria, South Africa*

[e] *School of Animal, Plant and Environmental Sciences, University of Witwatersrand, Private Bag X3, Johannesburg, 2050, South Africa*

Abstract

Remote sensing is crucial for producing accurate land use and land cover (LULC) maps. It provides continuous historical data, vital for sustainable development programs, where LULC is a crucial input criterion. Furthermore, natural carbon sinks like agriculture help reduce greenhouse gas emissions. Consequently, the primary objectives of this study are: 1) to monitor the LULC changes in the western Nile Delta, Egypt, spanning the period from 1985 to 2021; and 2) to quantify soil carbon sequestration (SCS) within the study area. In order to achieve these objectives, a supervised classification method was utilized, making use of eight Landsat satellite photos from the years 1985, 1990, 1995, 2000, 2005, 2010, 2015, and 2021. This approach aimed to detect patterns of LULC changes. Four distinct LULC categories were identified in the study area, namely agriculture, urban, bare land, and water. The findings unveiled a predominant transformation from bare land to agriculture, with approximately 3.8%, 5.4%, 6.4%, 13.4%, 23.6%, 24.3%, and 42.19% of bare land transitioning to agriculture during the periods of 1985-1990, 1990-1995, 1995-2000, 2000-2005, 2005-2010, 2010-2015, and 2015-2021, respectively. Furthermore, the analysis of SCS data indicated that soil carbon sequestration predominantly ranged from 440 to 2125 g/m^2, thereby highlighting the potential of the study area in terms of carbon storage. In conclusion, the analytical approach works efficiently for carbon sequestration evaluation. The study should be used to make land use decisions for carbon sequestration management.

Keywords: Land Use/ Land Cover, Change Detection, Carbon Sequestration, Remote Sensing, Western Nile Delta.

1. Introduction

Egypt's population has been steadily increasing, particularly in the past century. Most of this population growth has occurred in the densely populated Nile delta, which is considered one of the most crowded regions worldwide. The delta is home to approximately half of Egypt's population and encompasses about two-thirds of its cultivated land. After Nigeria and Ethiopia, Egypt ranks as the third most populous African country [1]. Consequently, successive governments have prioritized addressing the issue of overpopulation and its impact on the agriculture sector's continuous demand for increased agricultural production. As a result, Egyptian authorities have focused on reclaiming land and establishing new agricultural

* Corresponding author.
Email address: abdulahhelmy52@gmail.com (Abdullah H F Mohamed)

doi 10.21608/AELS.2024.247852.1044

Received: 19 December 2023, Revised: 2 March 2024
Accepted: 2 March 2024, Published: 3 March 2024

communities on the eastern and western fringes of the Nile delta, as well as other desert areas, particularly in the western desert. From 1997 to 2017, approximately 3.4 million feddans of cultivated land were added through land reclamation efforts in Egypt [2]. These development projects require careful monitoring to prevent large-scale environmental degradation caused by natural processes and human activities. Changes in land use/land cover (LULC) are major drivers of climate change [3]. Despite ongoing research on LULC change patterns, there remains an urgent need to develop fundamental datasets that provide quantitative and spatially explicit information on LULC changes [4]. Many countries are currently dealing with a serious environmental and climatic crisis as a result of the increase in anthropogenic greenhouse gases (GHG), particularly carbon dioxide (CO_2), in the atmosphere [5–8]. Therefore, it is crucial to quantify the impacts of LULC changes on CO_2 sources and sinks in the Western Delta [9]. Access to LULC information is essential for policymaking, business activities, and administrative purposes. Furthermore, such data, with their spatial details, are vital for environmental protection and spatial planning [4, 10]. Accurate land use classification is essential as it provides input data for environmental modeling, including climate change models and policy development [11]. Moreover, remotely sensed data obtained from orbiting satellites, with their repetitive coverage and consistent image quality, are particularly useful for change detection analysis [12]. Change detection involves identifying differences in the condition of an object or phenomenon by observing it at multiple time points [13–15]. It enables the quantification of temporal effects using multitemporal datasets [16]. Remote sensing (RS) technology is about to have a extensive impact on planning agencies and land management projects that track changes in land use and land cover at different spatial scales [17–19]. Furthermore, change detection has numerous applications related to LULC changes, such as shifting cultivation, land degradation and desertification, landscape changes, coastal changes, urban sprawl, urban landscape patterns, deforestation, quarrying activities, landscape fragmentation, and cumulative changes [20–22]. Therefore, there is an ongoing demand for accurate and up-to-date LULC information to support sustainable development programs, with LULC serving as a significant input criterion. Consequently, various research efforts have recognized the importance of adequately mapping LULC and tracking its changes over time to inform decision-making processes. For instance, land cover change assessment in urban environments and dynamic land cover monitoring have been applied [23, 24]. Change detection based on RS data has become an indispensable tool for providing comprehensive information to decision support systems for natural resource management and sustainable development. Consequently, assessing and mapping the current LULC situation and changes over time is critical for understanding and addressing social, economic, and environmental challenges [14, 24]. Even though many different change detection methods have been developed over the years, it is still hard to come up with the right one, especially for urban and fringe areas where factors are complicated and land uses quickly shift from rural to residential, commercial, industrial, and recreational [2].Carbon sequestration, particularly the capture and storage of CO_2, the most common GHG, is crucial for reducing atmospheric CO_2 levels and slowing down the rate of climate change [25, 26]. The United States Geological Survey (USGS) assesses two main types of carbon sequestration: geologic and biologic [27]. Carbon sequestration helps mitigate climate change by transferring additional carbon (C) from the atmosphere, primarily in the form of CO_2, to terrestrial biospheres like soil and vegetation, thereby limiting or shifting the increase in atmospheric CO_2 concentration [8]. Soil carbon sequestration refers to the increase in soil carbon content resulting from changes in management practices within the same landscape. This process traps additional carbon in the soil, separating it from other ecosystem components [28]. When a positive imbalance persists, the soil system eventually reaches a new, higher steady state of carbon stocks by removing CO_2 from the atmosphere. Enhanced soil organic carbon provides numerous benefits beyond miti-

gating climate change, including improved soil and water quality, ecological restoration, and increased crop yields [8]. One solution to mitigate CO_2 emissions is through carbon sequestration, which involves capturing and storing atmospheric carbon (C) in the terrestrial biosphere. Agricultural areas represent significant potential sinks and can absorb substantial amounts of carbon when trees are strategically integrated and managed alongside crops [27]. Numerous factors, including soil type, climate, topography, crop management, and anthropogenic activities, have an impact on the soil organic carbon pool (SOCP). SOCP is a critical global concern and a vital component of the United Nations Sustainable Development Goals (SDGs). LULC changes affect regional and global climate change through carbon emissions. Carbon sequestration can help replenish the carbon cycle and contribute to CO_2 emission reductions [29].

The primary objective of the study was to analyze changes in LULC within the study area using multitemporal remote sensing data. The study employed a supervised classification approach to monitor transformations in the western Nile Delta of Egypt across categories such as agricultural, urban, water, and bare land. The core focus was on identifying and quantifying changes from 1985 to 2021 by subtracting classified images from different years. Additionally, the study also estimated the soil carbon content in the study area as baseline information for any further carbon sequestration studies.

2. Material and methods

2.1. Study area

2.1.1. Location:

Delta, Egypt. It encompasses geographical coordinates between longitudes 30° 40 and 30° 40 E and latitudes 30° 8 and 30° 32 N (Fig. 1). With an approximate area of 2622 km (262,200 ha), the study area is predominantly part of the desert region within the Beheira governorate. However, it is important to small section in the southeast that belongs to the Giza governorate.

Figure 1. Location of the study area in the western Nile delta, Egypt.

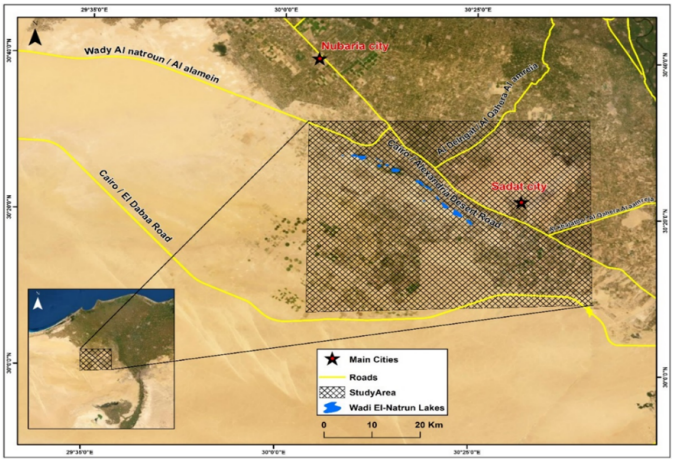

Figure 1: Location of the study area in the western Niledelta, Egypt

2.2. Soil description and Soil Carbon data collection:

The soils of Wadi El Natrun mainly consist of Sabkha formations located within desert depressions. The northern region's soil is predominantly sandy with calcareous crusts and sand dunes from the deltaic lacustrine complex. In contrast, the eastern area (El Sadat City) features gravel and gravelly sand soils associated with the deltaic phase, along with sand dunes. The southern region showcases gravely sand lithosols, accompanied by scattered patches of brown loamy soils in the desert [20]. The study area has undergone significant development as part of the western Nile Delta's land reclamation since the early 1980s. The Egyptian government's approach focuses on not only land reclamation but also sustainable village communities, addressing issues like unemployment and housing shortages. About 250,000 settlers and their families have benefitted from this project, with beneficiaries including unemployed graduates, former tenants, small farmers, and others [20].

For the current study, 18 soil samples were collected in July 2021 to assess and quantify soil carbon content, as shown in Table 8 and Figure 2. Samples were collected at a depth of 30 cm and stored in proper plastic bags to be sent to the lab for further analysis. Moreover, the geographic coordinates were recorded using a handheld device. The coordinates were collected for the soil carbon con-

tent mapping using the inverse distance-weighted (IDW) interpolation algorithm. Which determines pixel values using a linearly weighted combination of a set of sample points using the following equations:

$$w(x) = \frac{A}{B} \tag{1}$$

$$A = \sum_{i=1}^{n} \frac{1}{d(x,x_i)^p} ui \tag{2}$$

$$B = \sum_{i=1}^{n} \frac{1}{d(x,x_i)^p} \tag{3}$$

Where: w is the predicted value, d is the distance, x is the unknown point, x_i is the nth known point, ui is the value of the known point, and p is the power.

Carbon sequestration in grams per square meter was calculated using the following equation based [30].

$$C_s = 100 * OC * Bd * e \tag{4}$$

where: C_s = Organic Carbon Sequestration (g/m^2), OC = Organic Carbon (%), Bd = Soil Bulk Density (g/cm^3), and e = Depth of Sampling (cm) [30].

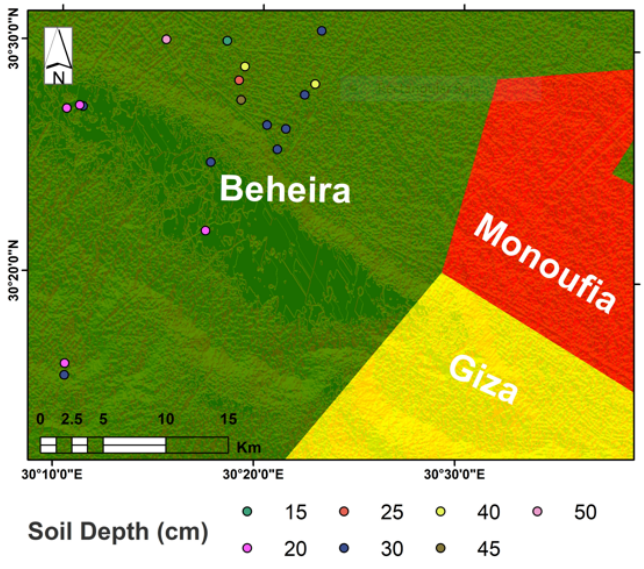

Figure 2: Soil samples sites in the study area

2.3. Climate

The meteorological data over the past four decades between 1981 and 2021 is represented in Table 1 (EMA). The average meteorological data of the climatic parameters of temperature (minimum, mean, maximum, range, and earth skin temperature at 2m, °C), wind speed (minimum, mean, maximum, and range at both 2m and 10m, m/s), precipitation (daily average, mm/day, and sum, mm), and humidity (relative, % and specific, g/kg at 2m). The monthly means of the climatic parameters were averaged over a total period of 40 years and shown in Table 1.

The study area belongs to the arid zone since the summation of annual precipitation is 48mm with zero precipitation during the summer months (July, August, and September). The minimum temperature of 4°C occurred during the winter months in January and February, besides the annual minimum temperature. The maximum temperature was 41.5°C in June and July, with a maximum annual temperature of 42.6°C. The mean temperatures are 12°C and 28°C in January and July, respectively, with an annual mean of 20.7°C. All average values for temperature at 2m height. The earth's skin temperature average ranged from around 12°C in January to 30°C in July and August, with an annual average of around 22°C.

The maximum wind speed generally increases in the winter months (January, February, and March) compared with the summer months. Additionally, the maximum wind speed at 10m is higher compared to the maximum wind speed at 2m. The average recorded maximum wind speed, at 2m, was 6.7 m/s in August, September, and October and increased to around 8 m/s from January to April. At 10m, the recorded maximum wind speed was around 9 m/s in August, September, and October and increased to around 11 m/s from January to April.

The relative humidity ranged from around 50 to 66.5% in May and January, respectively, with an annual average of around 59%. The surface pressure for all months is around 101 kPa.

Data source: Egyptian Meteorological Authority (EMA) and data reported by weather station: 623570, Latitude: 30.4 | Longitude: 30.35 | Altitude

Table 1: 1: The average climatic parameters between 1981 and 2021 in the study area

Parameter		JAN	FEB	MAR	APR	MAY	JUN	JUL	AUG	SEP	OCT	NOV	DEC	ANN
Temperature at 2m (°C)	Min	4.38	4.61	6.06	8.48	12.11	15.79	18.53	19.45	17.71	14.54	10.00	6.05	3.95
	Mean	12.22	13.04	15.61	19.55	23.46	26.55	27.91	28.06	26.18	22.86	18.27	14.01	20.68
	Max	22.92	26.43	31.46	37.33	40.19	41.49	41.03	40.10	38.80	35.67	30.10	24.72	42.59
Earth Skin Temperature (°C)		12.03	13.09	16.25	20.85	25.42	28.83	30.18	30.16	27.88	23.96	18.52	13.81	21.79
Wind Speed at 2m (m/s)	Min	0.19	0.25	0.21	0.23	0.25	0.33	0.43	0.38	0.32	0.25	0.21	0.20	0.06
	Mean	2.70	2.75	2.85	3.01	3.14	3.29	3.26	2.99	2.89	2.69	2.52	2.60	2.89
	Max	8.09	8.32	8.39	8.18	8.27	7.59	7.20	6.68	6.78	6.71	7.11	7.93	9.72
	Min	0.26	0.35	0.30	0.32	0.33	0.44	0.60	0.53	0.45	0.33	0.28	0.28	0.08
Wind Speed at 10m (m/s)	Mean	4.02	4.09	4.15	4.23	4.28	4.43	4.41	4.10	3.99	3.77	3.65	3.84	4.08
	Max	11.01	11.43	11.44	10.96	10.94	9.91	9.39	8.75	8.89	8.73	9.27	10.56	13.24
Relative Humidity at 2m (%)		66.50	62.88	59.62	52.58	50.28	51.66	55.06	57.14	58.50	61.60	63.98	66.18	58.83
Precipitation (mm/day)		0.44	0.38	0.36	0.25	0.05	0.01	0.02	0.00	0.01	0.14	0.34	0.33	0.19
Precipitation Sum (mm)		8.10	7.07	8.36	6.96	0.77	0.26	0.51	0.00	0.00	2.62	7.26	5.92	47.84

Data source: EgyptianMeteorological Authority (EMA) and data reported by weather station: 623570,Latitude: 30.4 | Longitude: 30.35 | Altitude

2.4. Remote sensing data:

The study utilized a dataset of eight Landsat satellite images, spanning 36 years, acquired on specific dates detailed in Table 2. It includes Landsat 5 images for 1985, 1990, 1995, 2005, and 2010; Landsat 7 for 2000; and Landsat 8 (OLI) for 2015 and 2021. These images are freely accessible from the USGS-managed Landsat archive through links: http://glovis.usgs.gov and http://edcsns17.cr.usgs.gov. The images have Universal Transverse Mercator projection (zone 36N, datum WGS-84), with a 30m x 30m spatial resolution. Acquired in summer to minimize cloud cover, they capture distinct spectral variations among agricultural fields, bare land, and urban areas. The analysis used all available Landsat image bands and supplemented the image classification with archived data, sketch maps, and Google Earth references.

Characterization of Satellite data sets for the study area

Data source: United States Geological Survey (USGS)

2.5. Image enhancement and visual interpretation:

Image enhancement involves altering image values to emphasize information within the picture and enhance its visual interpretability by augmenting distinctions between features. This approach aims to optimize the collaborative strengths of human cognition and computational processing. Typically, these improved images find utility in visual assessments, while the unaltered originals serve automated analyses. In this study, prior to image classification, LULC features are classified according to established methodologies [17, 18, 31].

2.6. Image classification:

The ArcGIS software facilitates the digital image processing of the Landsat image sets mentioned earlier. The classification process was achieved using the supervised maximum likelihood classifier tool. Representative sites set up training samples for predetermined types of LULC. These are done by using enclosed polygon pixels to find spectral signatures that are unique to each type based

Table 2: Characterization of Satellite data sets for thestudy area

Acquired date	Spacecraft/Sensor	Path/Row	Pixel Size (m)	Coordinate System/Datum
7/12/1985	LANDSAT_5/TM	177/39	30	UTM/WGS 84
7/10/1990	LANDSAT_5/TM	177/39	30	UTM/WGS 84
7/8/1995	LANDSAT_5/TM	177/39	30	UTM/WGS 84
7/13/2000	LANDSAT_7/ETM	177/39	30	UTM/WGS 84
7/3/2005	LANDSAT_5/TM	177/39	30	UTM/WGS 84
7/17/2010	LANDSAT_5/TM	177/39	30	UTM/WGS 84
7/15/2015	LANDSAT_8/OLI	177/39	30	UTM/WGS 84
7/15/2021	LANDSAT_8/OLI	177/39	30	UTM/WGS 84

Data source: United StatesGeological Survey (USGS)

on records from satellite images. Spectral signatures aim for minimal confusion between mapped land covers. This method yields a thematic raster layer (classified image) and a distance file [8, 19–23, 27, 29, 31].

2.7. Change detection:

Change detection is a prevalent remote sensing approach that involves comparing multiple images of the same area taken at different times to identify alterations in specific image attributes. Authors have widely embraced digital change detection techniques, encompassing a variety of remotely sensed data and methodologies, including newer emerging methods. For instance, [35] presented diverse change detection techniques applicable to synthetic aperture radar (SAR) and optical images. They assessed various aspects of this process, such as data pre-processing, change detection generation, and techniques employed [14, 32].

3. Results and discussion

3.1. The classification accuracy assessment

Maximum likelihood showed better classification results than other classification algorithms. The overall accuracies and Kappa coefficients of all classification algorithms improved progressively from TM (1985,1990, and 1995) and ETM (2000, 2005, and 2010) toward OLI (2015 and 2021). This can be attributed to the fact that the fifth data set (OLI 2015 and 2021) was acquired closer in time to the collection of training and validation points.

As presented in Tables 3, 4 and 5, the results of accuracy assessment were 83%, 85%, 83%, 85%, 82%, 86%, 92% and 92%, for the years of 1985, 1990, 1995, 2000, 2005, 2010, 2015, and 2021, respectively.

3.2. Land use/cover Classes area as obtained from the classification

The data presented in Table 4 represent the total area of each LULC category for each study year (1985, 1990, 1995, 2000, 2005, 2010, 2015, and 2021), respectively. In 1985, as presented in Figure 6 and Table 3, barren land was the largest class, representing 2518.52 km^2 of the total LULC categories assigned. The area of agriculture class had increased significantly; after being about 51.55 km^2 in 1985, it now occupies about 927.50km^2 of the study area in 2005. In 2021, the percentage of the agriculture class had doubled significantly again, resulting in the agriculture class becoming the largest class, occupying 1733.95 km^2 of the study area.

In 1985, Figure (4a) illustrates the dominant land class in the study area, with "barren class" occupying the largest extent. This class accounted for 96% of the total land use and land cover (LULC) classes, covering an area of 2518.5 km2. On the contrary, the "agriculture" class remained relatively small, comprising only 51.5 km2, which represented 1.9% of the study area. This limited coverage can be attributed to the scarcity of agricultural investment projects during that period. The "water" class encompassed 10.9 km2, equating to 0.41% of the

Table 3: Accuracy assessment for the years of 1985, 1990and 1995

	1985	Reference data					
	Class	Bare Land	Agriculture	Urban	Water	Total	User Accuracy
Classification	Bare Land	163	3	27	3	196	83.16%
	Agriculture	5	109	5	1	120	90.83%
	Urban	20	8	73	3	104	70.19%
	Water	3	5	2	70	80	87.50%
	Total	191	125	107	77	500	82.92%
	Producer Accuracy	85.34%	87.20%	68.22%	90.91%	82.92%	83.00%
	Overall Accuracy	83.00%					
	1990	Reference data					
	Class	Bare Land	Agriculture	Urban	Water	Total	User Accuracy
Classification	Bare Land	143	7	14	0	164	87.20%
	Agriculture	8	120	5	1	134	89.55%
	Urban	12	8	85	3	108	78.70%
	Water	3	3	7	81	94	86.17%
	Total	166	138	111	85	500	85.41%
	Producer Accuracy	86.14%	86.96%	76.58%	95.29%	86.24%	85.80%
	Overall Accuracy	85.80%					
	1995	Reference data					
	Class	Bare Land	Agriculture	Urban	Water	Total	User Accuracy
Classification	Bare Land	156	3	15	3	177	88.14%
	Agriculture	5	130	3	12	150	86.67%
	Urban	19	8	60	6	93	64.52%
	Water	3	5	2	70	80	87.50%
	Total	183	146	80	91	500	81.70%
	Producer Accuracy	85.25%	89.04%	75.00%	76.92%	81.55%	83.20%
	Overall Accuracy	83.20%					

Table 4: Accuracy assessment for the years of 2000, 2005,and 2010

	2000	Reference data					
	Class	Bare Land	Agriculture	Urban	Water	Total	User Accuracy
Classification	Bare Land	144	3	14	4	165	87.27%
	Agriculture	5	127	5	2	139	91.37%
	Urban	15	8	56	4	83	67.47%
	Water	3	5	6	99	113	87.61%
	Total	167	143	81	109	500	83.43%
	Producer Accuracy	86.23%	88.81%	69.14%	90.83%	83.75%	85.20%
	Overall Accuracy	85.20%					
	2005	Reference data					
	Class	Bare Land	Agriculture	Urban	Water	Total	User Accuracy
Classification	Bare Land	138	12	17	0	167	82.63%
	Agriculture	5	100	7	3	115	86.96%
	Urban	25	11	78	5	119	65.55%
	Water	0	3	2	94	99	94.95%
	Total	168	126	104	102	500	82.52%
	Producer Accuracy	82.14%	79.37%	75.00%	92.16%	82.17%	82.00%
	Overall Accuracy	82.00%					
	2010	Reference data					
	Class	Bare Land	Agriculture	Urban	Water	Total	User Accuracy
Classification	Bare Land	109	3	11	3	126	86.51%
	Agriculture	15	143	5	0	163	87.73%
	Urban	8	10	92	3	113	81.42%
	Water	0	7	2	89	98	90.82%
	Total	132	163	110	95	500	86.62%
	Producer Accuracy	82.58%	87.73%	83.64%	93.68%	86.91%	86.60%
	Overall Accuracy	86.60%					

Table 5: Accuracy assessment for the years of 2015, and 2021

	2015	Reference data					
	Class	Bare Land	Agriculture	Urban	Water	Total	User Accuracy
Classification	Bare Land	123	3	7	2	135	91.11%
	Agriculture	5	160	4	0	169	94.67%
	Urban	5	7	82	5	99	82.83%
	Water	3	3	2	89	97	91.75%
	Total	136	173	95	96	500	90.09%
	Producer Accuracy	90.44%	92.49%	86.32%	92.71%	90.49%	90.80%
	Overall Accuracy	90.80%					
	2021	Reference data					
	Class	Bare Land	Agriculture	Urban	Water	Total	User Accuracy
Classification	Bare Land	97	1	9	0	107	90.65%
	Agriculture	5	167	4	2	178	93.82%
	Urban	9	3	102	1	115	88.70%
	Water	3	2	1	94	100	94.00%
	Total	114	173	116	97	500	91.79%
	Producer Accuracy	85.09%	96.53%	87.93%	96.91%	91.61%	92.00%
	Overall Accuracy	92.00%					

Table 6: Displays the areas of different land use and land cover classes as determined by the classification process.

Classes	Area (km^2)							
	Agriculture		Bare land		Urban		Water	
	Km ^{2}	%	Km ^{2}	%	Km ^{2}	%	Km ^{2}	%
1985	51.5	1.9	2518.5	96	41.4	1.5	10.9	0.41
1990	146.8	5.6	2423.9	92.4	44.5	1.6	7.2	0.27
1995	255.3	9.7	2310.8	88.1	45.4	1.7	10.9	0.41
2000	466.2	17.7	2030.2	77.4	112.1	4.2	11.4	0.43
2005	927.5	35.3	1542.05	58.8	139.6	5.3	10.8	0.41
2010	1148.11	43.6	1146.6	43.7	319.06	12.1	8.6	0.33
2015	1304.8	49.7	1011.08	38.5	299.2	11.4	7.2	0.27
2021	1734	66.1	634.08	24.1	247.0	9.4	7.3	0.28

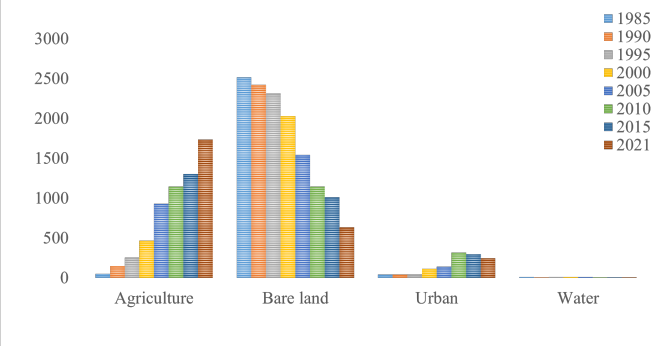

Figure 3: LULC different classes area (km2) in the investigated year

study area, while the "urban" class occupied 41.4 km2, constituting 1.5% of the total study area.

Figure (4b) illustrates notable changes in land cover classes between 1985 and 1990. The agriculture class experienced a significant increase, doubling from approximately 1.9% and covering an area of 2518.5 km2 in 1985 to occupying about 6.2% and representing 146.8 km2 of the study area in 1990. This growth can be attributed to the government's increased focus on agricultural land reclamation projects in the Wadi El-Natrun area.

In contrast, the bare land class witnessed a decline from around 96% in 1985 to 92.4% in 1990, representing an area of 2423.9 km2. This decrease of 4.5% was a result of agricultural development initiatives.

Simultaneously, the urban class expanded slightly, with its coverage increasing from 41.4 km2 (1.5% of the study area) in 1985 to 44.5 km^2 (1.6% of the study area) in 1990.

Furthermore, the water class experienced a decrease, shrinking from 10.9 km2 (0.41% of the study area) in 1985 to 7.7 km^2 (0.27% of the study area) in 1990.

Figure (4c) illustrates significant changes in land cover classes during the period of 1995. The agriculture class experienced another notable increase, doubling from approximately 5.6% and covering an area of 146 km2 in 1990 to occupying 9.7% and 255.4 km2 of the study area in 1995. This expansion indicates a continued focus on agricultural development projects, resulting in the conversion of other land cover types to agricultural land.

Consequently, the bare land class witnessed a decline, decreasing to approximately 88% and covering an area of 2310.8 km^2.

Moreover, the water class experienced an increase, rising from representing 0.27% of the total study area in 1990 to 0.41% in 1995.

Additionally, the urban class exhibited a slight increase, with its coverage expanding from 1.6% in 1990 to 1.7% in 1995. This growth suggests urbanization trends and the expansion of built-up areas over time.

Figure (4d) depicts substantial changes in the study area, particularly the transformation of large areas from the bare land class to the agricultural class. The agriculture class experienced a remarkable increase of 15.8% between 1985 and 2000. In 2000, it occupied 17.7% of the study area, covering an expansive 466 km^2. This significant expansion

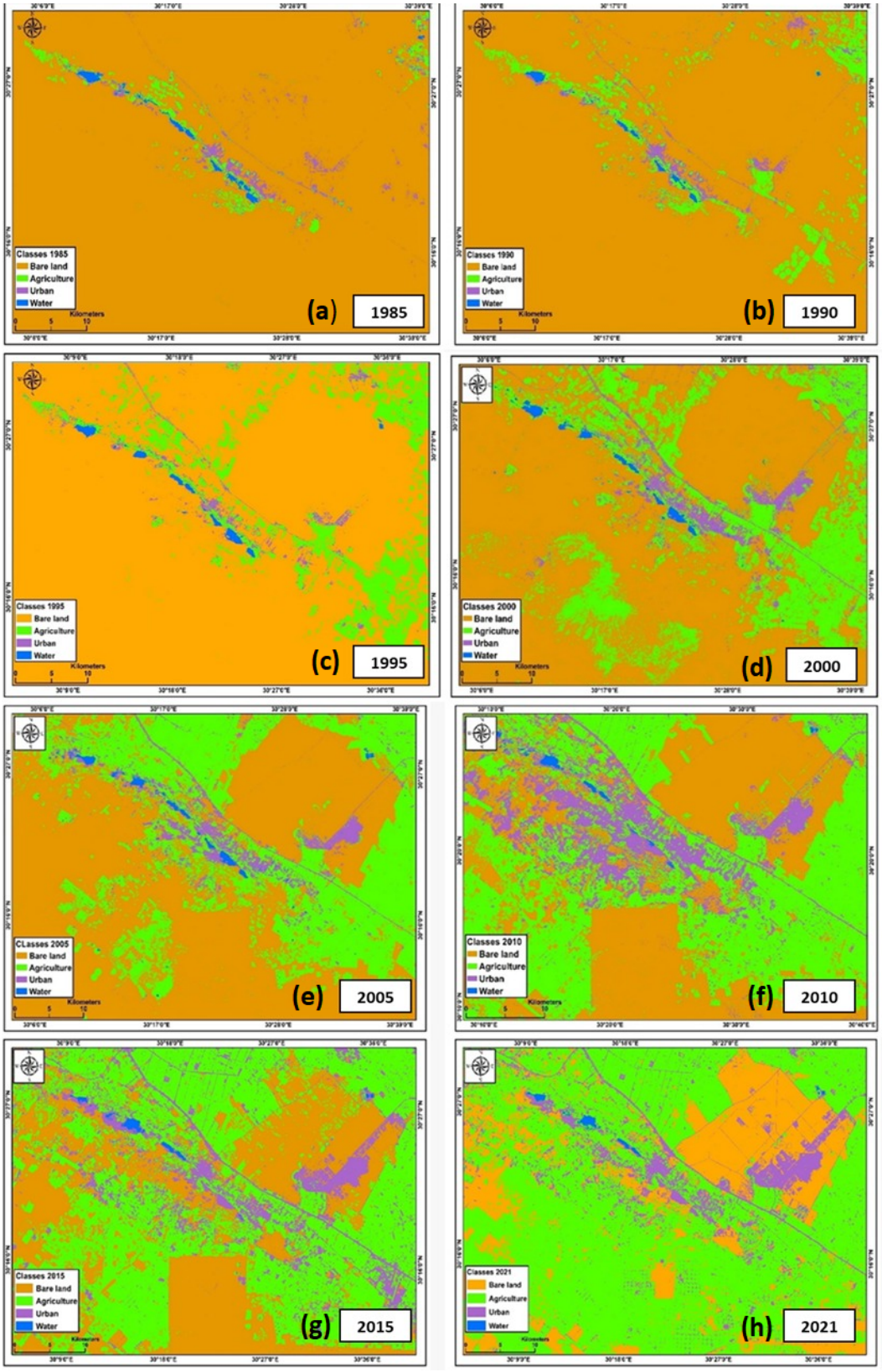

Figure 4: Land use and land cover maps produced by the supervised classification.

highlights the successful implementation of agricultural reclamation projects, leading to the conversion of previously barren land into productive agricultural areas.

There is a noticeable expansion of the urban class in contrast to the total area of bare land. The urban class's coverage increased from 1.5% in 1985 to 4.2% in 2000. This expansion signifies the growth of urban areas and the conversion of land for residential, commercial, and infrastructural purposes. Consequently, the bare land class decreased to approximately 77.4% in 2000, a significant decline from its dominance of 96% in 1985.

Overall, Figure (4d) portrays a dynamic landscape where the bare land class underwent substantial changes, with a significant portion being converted into agricultural land. The expansion of the urban class demonstrates the ongoing urbanization processes in the study area.

Figure (4e) demonstrates significant changes in the study area, particularly regarding agriculture and bare land classes. The agriculture class underwent another substantial increase, doubling from occupying 17.7% and covering 466 km^2 in 2000 to representing 35.3% and encompassing 927 km^2 in 2005. This significant expansion highlights the continued success of agricultural development initiatives, resulting in the conversion of additional land into productive agricultural areas.

Conversely, the bare land class witnessed a notable decline, decreasing from 77.4% and covering 2030 km2 in 2000 to 58.8% and 1542 km^2 in 2005.

Moreover, Figure (4e) reveals a noticeable expansion of the urban class in relation to the total area of bare land. The urban class coverage increased from 4.2% in 2000 to 5.3% in 2005.

Additionally, the water class experienced a decline, decreasing to approximately 0.41% in 2005 from its dominance of 0.43% in 2000.

In summary, Figure (4e) depicts significant shifts in land cover classes, with a substantial increase in agriculture, a corresponding decline in bare land, an expansion of urban areas, and a decrease in the water class. These changes reflect the ongoing agricultural and urban development as well as potential alterations in hydrological patterns within the study area during the specified period.

Figure (4f) illustrates the land use and land cover maps resulting from supervised classification in 2010, providing insights into notable changes. The most significant transformation occurred in the urban class, which experienced a doubling in coverage. It expanded to represent 12.1% of the study area, covering 319 km2, compared to approximately 5.3% and 139 km2 in 2005.

Additionally, there was a noticeable expansion in the agricultural class, which increased to 1145.5 km2, representing 43.6% of the study area in 2010. In 2005, it covered approximately 927.5 km2, accounting for 35.3% of the area.

This increase in agricultural land was directed against the total area of bare land, indicating the conversion of bare land into agricultural areas.

The bare land class in 2010 covered 1146.7 km2, representing 43.7% of the study area. This marked a decrease from its coverage of approximately 1542 km2, accounting for 58.8% in 2005.

Furthermore, the water class witnessed a decline, occupying 0.33% in 2010 compared to 0.41% in 2005. Changes in hydrological conditions, land use patterns, or human interventions that affect water bodies may all have an impact on this decrease.

In summary, Figure (4f) indicates significant changes in land use and land cover patterns. The urban class expanded, while the agricultural class increased at the expense of bare land. The decrease in the water class suggests potential alterations in the hydrological landscape. These changes reflect the dynamics of urbanization, agricultural development, and potential environmental shifts within the study area during the specified period.

Figure (4g) portrays the changes in land use and land cover in 2015, revealing several noteworthy observations. Firstly, there was a slight increase in the agriculture class compared to 2010. In 2010, the agriculture class accounted for about 43.6% of the area, covering 1145.5 km^2. However, in 2015, it expanded to represent 49.7% of the area, encompassing 1304 km^2.

Conversely, the bare land class exhibited a decrease in coverage. In 2010, the bare land class accounted for 1146.7 km^2, comprising 43.6% of the area. However, by 2015, it had decreased to 38.5%

of the area, covering 1012 km^2. This decline suggests a conversion of bare land into other land cover classes, such as agricultural or urban areas.

Moreover, the total area of the water class experienced a slight decrease. It diminished to 7.2 km2 in 2015 from 8.6 km2 in 2010.

Additionally, the urban class witnessed a slight decrease in coverage. In 2015, it accounted for approximately 11.4% of the area, while in 2010, it represented 12.1%. This indicates a relatively slower pace of urban expansion during the specified period, potentially influenced by factors such as urban planning, land use regulations, or economic factors.

In summary, Figure (4g) highlights a slight increase in the agriculture class, a decrease in the bare land class, a slight decrease in the total area of the water class, and a slight decrease in the urban class in 2015 compared to 2010. These changes reflect the dynamic nature of land use and land cover patterns, influenced by various factors such as agricultural development, land management practices, water dynamics, and urbanization processes within the study area during the specified period.

Figure (4h) reveals several significant land use changes between the years 2015 and 2021. The land use change analysis technique detected additional loss in the total area of bare land, which decreased to nearly 24% in 2021 compared to approximately 38.5% in 2015. This indicates a substantial reduction in bare land cover within the specified period.

On the other hand, the agriculture class experienced an increase in coverage. In 2015, it occupied 49.7% of the area, but by 2021, it expanded to cover approximately 66.1%.

Moreover, there was a decrease in the urban class. In 2015, the urban class accounted for 11.4% of the area, but by 2021, it had decreased to 9.4%. Furthermore, there was a slight increase in the water class, which occupied 0.28% in 2021 compared to the same percentage in 2015.

3.3. Change Detection results

The presented data in Table 6 and Figure 4 provide information on the total area of each land use and land cover (LULC) category for specific study years (1985, 1990, 1995, 2000, 2005, 2010, 2015, and 2021). Additionally, Figure 3 displays the area (in km^2) of different LULC classes during the investigated years. The spatial distribution of these categories can be observed in Figures 5 and 6.

In 1985, barren land constituted the largest class, covering 96% (2518.52 km^2) of the assigned LULC categories. However, the agriculture class experienced significant growth during the study period. It started at 1.9% (51.55 km^2) in 1985 and expanded to occupy approximately 35% (927.50 km^2) of the study area by 2005. By 2021, the percentage of the agriculture class had doubled once again, making it the largest class, covering 66% (1733.95 km^2) of the study area.

This substantial increase in agricultural land can be attributed to land reclamation projects carried out between 1985 and 2005.

The implementation of these projects likely contributed to the expansion of agricultural areas. This trend continued between 2005 and 2021, resulting in the dominance of the agriculture class in the study area.

It is important to note that the detailed spatial distribution of the LULC categories can be observed in Figures 5 and 6, providing further insights into the patterns and changes in land use and land cover over time.

3.4. Nature and location of changes in LULC

rovides information on the change detection status, percentages of changed areas, and the rate of change in each land use and land cover (LULC) class. The location of these changes is depicted in the maps presentedin Figures 5 and 6. Analysis of the data in Table 6 and Table 7 revealed moderate to slight undesirable long-term changes, including conversions from agricultural land to barren land and urban areas.

The total long-term change rate indicates a significant increase in agricultural land from 1985 to 2021, reaching almost 66%. In contrast, there was a decrease in the change rate of barren land by approximately 24% during the same period. These changes can be attributed to the implementation of land reclamation projects in the study

Table 7: LULC Change Detection summary.

Classes	Area (Km^2)			
	Agriculture	Bare land	Urban	Water
1985	51.55	2518.52	41.44	10.96
1990	146.80	2423.89	44.55	7.23
Change (1990: 1985)	95.25	-94.63	3.11	-3.73
1995	255.33	2310.78	45.42	10.94
Change (1995 - 1990)	108.53	-113.11	0.87	3.71
2000	466.73	2030.17	112.17	11.40
Change (2000 - 1995)	213.40	-280.61	66.75	0.46
2005	929.91	1542.05	139.69	10.82
Change (2005-2000)	461.18	-488.12	27.52	-0.58
2010	1148.11	1146.62	319.06	8.68
Change (2010-2005)	218.20	-395.43	179.37	-2.14
2015	1304.87	1011.08	299.28	7.24
Change (2015-2010)	156.76	-135.54	-19.78	-1.44
2021	1733.98	634.08	247.02	7.39
Change (2021-2015)	429.11	-377.00	-52.26	0.15
Change (2021 - 1985)	1682.40	-1884.29	205.58	-3.57
Classes	**changepercentage (%)**			
	Agriculture	Bare land	Urban	Water
1990 - 1985	184.8	-3.8	7.5	-34.0
1995 - 1990	73.9	-4.7	2.0	51.4
1995 - 2000	82.5	-12.1	147.0	4.2
2000 - 2005	98.9	-24.0	24.5	-5.1
2005 - 2010	23.5	-25.6	128.4	-19.8
2010 - 2015	13.8	-11.7	-6.2	-16.6
2015 - 2021	33.0	-37.3	-17.5	2.0

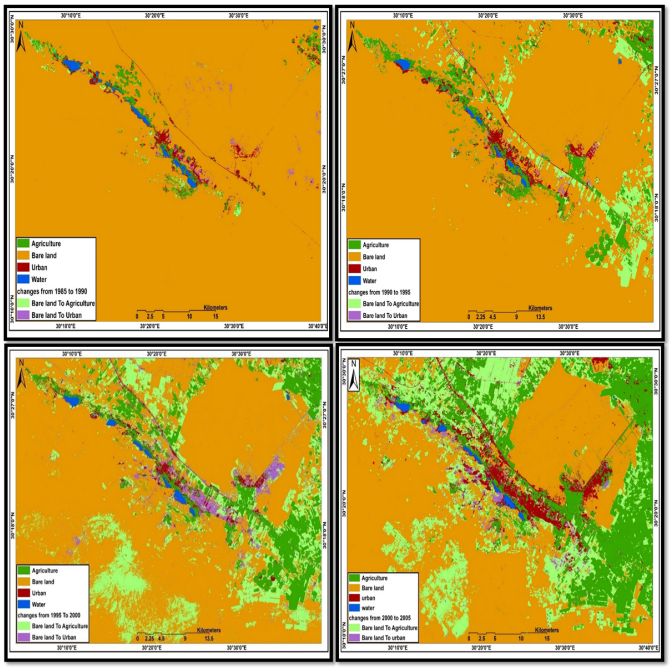

Figure 5: The spatial distribution ofLULC change occurred between (1985 to 1990), (1990 to 1995), (1995 to 2000) and(2000 to 2005)

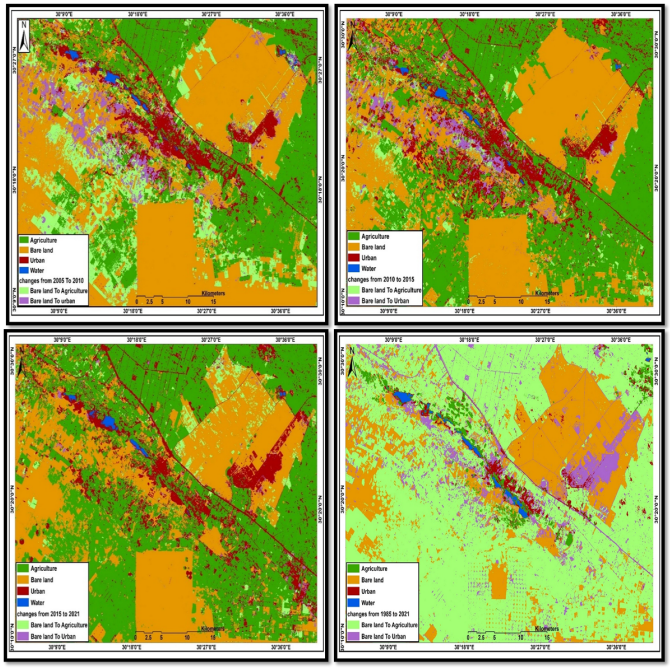

Figure 6: The spatial distribution of LULCchange occurred between (2005 to 2010), (2010 to 2015), (2015 to 2021) and (1985 to 2021)

area, which facilitated the expansion of agricultural land.

Comparing the periods 1985 –2000 and 2000 –2015, it was observed that the rate of expansion in the urban class significantly increased in the latter period. The percentage change in the urban class was 1.5%, 1.6%, 1.7%, 4.2%, 5.3%, 12.1%, 11.4%, and 9.4% for the years 1985, 1990, 1995, 2000, 2005, 2010, 2015, and 2021, respectively. This substantial increase in the urban class is likely attributed to the expansion of residential allotments and industrial areas since 2005.

Regarding the water class, the results of image classification indicated several increases from 1985 to 2000, where it occupied 10.9 km2 in 1985 and expanded to 11.4 km^2 in 2000. However, from 2000 to 2021, there was a significant decrease, with the water class covering 7.3 km2 in 2021. The decrease in the water class is a result of hydrological changes that lead to fluctuations in the underground water levels, consequently affecting the lakes of Wadi El-Natron.

In summary, Table 7 provides insights into the change detection status and rates of change in each LULC class. The maps in Figures 5 and 6 illustrate the spatial distribution of these changes. The findings highlight the increase in agricultural land and decrease in barren land, the significant expansion of the urban class, and the changes in the water class over the study period. Government policies regarding water bodies, urbanization, and land reclamation initiatives are some of the factors that affect these changes.

3.5. Soil Carbon Sequestration:

In this study, the soil carbon sequestration (SCS) was calculated in the study area as a baseline. As shown in Figure 7, The SCS results indicated that the sequester carbon in the soil ranged mostly from 440 to 2125 g/m2.

These findings underscore the potential of agricultural activities to mitigate greenhouse gas emissions and enhance carbon sequestration in the research area. Effective carbon sequestration not only prevents the release of CO2 into the atmosphere but also aids in the removal of existing CO2, resulting in a direct decrease in atmospheric concentrations. This decline in CO2 levels generates a positive feedback effect by diminishing the greenhouse effect and subsequently decelerating global warming. The findings of this research will improve our understanding of the crucial role that carbon sequestration plays in addressing climate change and provide useful insights into the potential benefits and difficulties associated with its widespread implementation.

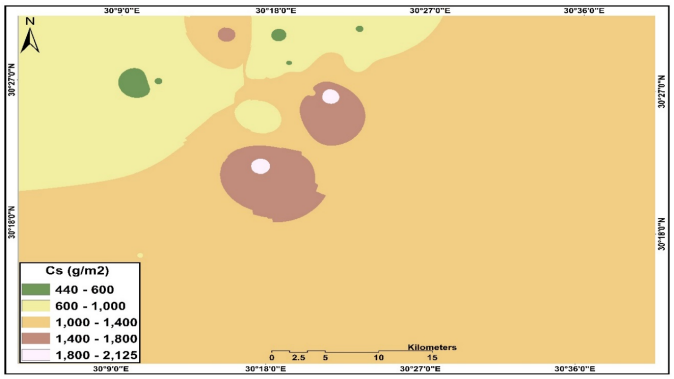

Figure 7: Carbonsequestration in grams per square meter in the study area

The adoption of effective carbon sequestration methods may hold significant potential substantially reducing CO emissions and contributing to global endeavors [30].

Figure 7. Carbon sequestration in grams per square meter in the study area

4. DISCUSSION

Egypt's population has been steadily increasing, particularly in the past century. Most of this population growth has occurred in the densely populated Nile delta, which is considered one of the most crowded regions worldwide [1]. Consequently, successive governments have prioritized addressing the issue of overpopulation and its impact on the agriculture sector's continuous demand for increased agricultural production [2]. Accordingly, these development projects require careful monitoring to prevent large-scale environmental degradation caused by natural processes and human activities.

Table 8: Soil parameters for subsurface horizon in the studied area at Western Delta.

ID	Depth (cm)	Bulk Density (g/cm^3)	OC (%)	Cs (g/m^2)	Lu/Lc class	Soil type
S1	20	1.80	0.12	439.53	Agriculture	coarse sand
S2	30	1.58	0.10	496.05	Agriculture	coarse sand
S3	20	1.42	0.29	825.58	Agriculture	Medium sand
S4	20	1.60	0.58	1860.47	Agriculture	Fine sand
S5	20	1.62	0.30	979.53	Agriculture	Medium sand
S6	30	1.62	0.15	706.40	Agriculture	Medium sand
S7	30	1.63	0.26	1279.36	Agriculture	Medium sand
S8	50	1.61	0.18	1472.88	Agriculture	Fine sand
S9	30	1.67	0.28	1382.09	Agriculture	medium sand
S10	30	1.62	0.35	1718.37	Agriculture	Fine sand
S11	30	1.66	0.43	2128.44	Agriculture	Fine sand
S12	40	1.65	0.14	897.54	Agriculture	Medium sand
S13	45	1.62	0.15	1088.81	Agriculture	Medium sand
S14	40	1.64	0.15	954.66	Agriculture	Medium sand
S15	15	1.63	0.21	512.37	Agriculture	coarse sand
S16	30	1.68	0.12	587.48	Agriculture	coarse sand
S17	30	1.60	0.23	1084.75	Agriculture	Medium sand
S18	25	1.64	0.14	557.56	Agriculture	coarse sand

The analysis of land use and land cover (LULC) change patterns in the western Nile Delta of Egypt revealed several significant transformations. The predominant change observed over the study period was the conversion of bare land to agriculture. This conversion occurred progressively, with a substantial increase in agricultural land between 1985 and 2021. The findings indicate a continuous expansion of agricultural activities in the region, likely driven by land reclamation efforts and the increasing demand for agricultural production due to population growth. The observed changes in LULC provide valuable insights into the dynamics of land transformation and the implications for environmental management and sustainable development in the study area.

Remote sensing and image classification techniques played a crucial role in detecting and analyzing LULC changes over the study period. The use of Landsat satellite data and a supervised classification approach allowed for the accurate identification and mapping of different land cover categories, including agriculture, urban areas, bare land, and water bodies [1]. The availability of historical Landsat images spanning several decades enabled the assessment of long-term LULC dynamics. The findings demonstrate the effectiveness of remote sensing as a tool for monitoring and understanding land-use changes, providing valuable information for land management strategies and decision-making processes [11].

Our ability to forecast and mitigate the consequences of climate and land cover changes relies, in part, on a precise description of the distribution of soil organic carbon (SOC) and carbon stocks (CS), as well as an understanding of the factors influencing the inputs and outputs of SOC [33, 34]. Moreover, investigating land use and land cover (LULC) changes and their spatial distribution, along with the content of carbon stocks, is crucial for examining the global carbon cycle and the greenhouse effect [35–37]. Consequently, it is essential to quantitatively assess the impacts of LULC changes on carbon dioxide (CO2) sources and sinks in the Western Delta [9]. As presented in Figure 3 and Table 6, in 1985, barren land was the largest class, representing 2518.52 km^2 of the total LULC categories assigned. The area of agriculture

class had increased significantly; after being about 51.55 km^2 in 1985, it occupied about 927.50km^2 of the study area in 2005. The increase in agriculture class that occurred at the expense of the decrease in bare land class can be attributed to the continuous expansion of agricultural reclamation projects in the study area, which aimed to maximize land utilization and increase agricultural productivity to provide food security for the continued population growth.

In 2021, the percentage of the agriculture class had doubled significantly again, resulting in the agriculture class becoming the largest class, occupying 1733.95 km^2 of the study area.

The total long-term change rate of the increase in agricultural land (from 1985 to 2021) increased to almost 66%, in contrast to a decrease in the change rate of barren land by approximately 24% in the same period.

The number of agricultural land reclamation projects doubled by in these periods as a result of the country's interest in agricultural development in the study area and its plans to achieve food security by encouraging agricultural investment companies to invest in this area and providing a lot of facilities to these companies. And this interest came for many reasons. For example, Egypt has a rapidly growing population, and with that comes the need to produce more food to meet the increasing demand. This necessitates the expansion of agricultural land to maximize food production [2]. Furthermore, from an economic importance viewpoint, agriculture plays a crucial role in the Egyptian economy, employing a significant portion of the population and contributing to the country's export earnings. Increasing agricultural land helps enhance productivity and boost the agricultural sector's contribution to the national economy [1].

Agricultural policy and incentives: The Egyptian government has implemented various policies and incentives to encourage agricultural expansion. These include providing subsidies, facilitating access to credit, and offering support to farmers in terms of infrastructure and irrigation systems. These measures have encouraged farmers to convert bare land into agricultural land [38].

Land reclamation projects: Egypt has undertaken extensive land reclamation projects to convert barren or marshy areas into productive agricultural land. These projects involve draining waterlogged areas, building dykes to control flooding, and applying techniques like soil improvement, leveling, and proper drainage systems [39].

Agricultural development programs: Various agricultural development programs and initiatives are implemented to enhance productivity and increase crop yields. This often involves converting bare land into cultivated fields to maximize agricultural output [39].

Compared to the period 1985-2000, the period 2000-2015 witnessed a huge increased in the rate of expansion in the urban class. The classification result by percentage of the change in the urban class was 1.5%, 1.6%, 1.7%, 4.2%, 5.3%, 12.6 %, and 11.4%, respectively. This was probably due to the increased expansion rate that has happened in residential allotments and industrial areas since 2005. This growth indicates ongoing urbanization processes and the conversion of bare land class for urban development, including residential, commercial, and infrastructure projects to meet the increase in agricultural and industrial projects.

Within the period from 1985 to 2021, minor changes occurred in the water class. These changes may be attributed to factors such as changes in hydrological conditions affecting water bodies during the specified timeframe.

The results of image classification and LULC change detection indicated that an intensive development program has been implemented in the study area during the last four decades. Developments within the study area include land reclamation and the expansion of irrigated areas into the desert, as well as the establishment of many rural, industrial, and commercial communities. All of these (bio) physical changes within the setting of the region's ecosystems reflect the dynamics of human impacts on the study area.

Soil organic carbon (SOC) plays a crucial role in soil sustainability, fertility, degradation, and crop production. When considering a large-scale context and monitoring SOC, soil properties have been utilized as effective tools to assess the impact of land use change on SOC levels. [40–42].

The estimation of carbon (C) emissions resulting from land-use changes involves applying carbon sequestration and soil organic carbon (SOCP) assessments to soil profiles [43, 44].

The study investigated the impact of LULC change on soil carbon sequestration (SCS) in the western Nile Delta, as shown in Figure 7. The results indicate that the sequestered carbon in the soil varied within a range of 440 to 2125 g/m^2. This indicates the capacity of the study area to act as a carbon sink, contributing to the mitigation of greenhouse gas emissions. The conversion of bare land to agriculture, which accounted for a significant proportion of the observed LULC changes, likely contributed to increased carbon sequestration in the soil. Agricultural practices, such as the cultivation of crops and the application of organic matter, can enhance carbon storage in the soil [45]. These findings highlight the potential of agricultural activities as a means to mitigate greenhouse gas emissions and promote carbon sequestration in the study area.

The implementation of efficient carbon sequestration methods holds tremendous potential for combating rising atmospheric CO_2 concentrations. By capturing CO_2 from industrial processes, power plants, and other emission sources, and storing it in stable carbon sinks, such as agricultural land and geological formations. Effective carbon sequestration not only prevents the release of CO_2 into the atmosphere but also facilitates the removal of CO_2 already present, leading to a direct decrease in atmospheric concentrations [46]. This reduction in CO_2 levels has a positive feedback effect, as lower concentrations result in a diminished greenhouse effect and a subsequent slowdown in global warming.

The insights gained from this study have important implications for environmental management and policy development in the western Nile Delta. The observed trends in land use change and carbon sequestration highlight the need for sustainable land management practices that balance agricultural expansion with environmental conservation.

Future research efforts could focus on evaluating the ecological and socio-economic impacts of LULC changes, investigating the effectiveness of different land management strategies in promoting carbon sequestration, and assessing the resilience of the region's ecosystems to ongoing environmental changes. Such research is essential for informing targeted policies and interventions aimed at achieving sustainable development goals and mitigating the adverse effects of climate change in the study area [27].

In finale, the present study has provided basic data for one of the most important Egyptian agriculture regions, which in turn will offer scientific guidance for policy making efforts to improve agriculture practices and control CO_2 emissions in Egypt.

5. Conclusion

It can be concluded from this study that the combination of GIS and remote sensing data, known as RS&GIS, is a valuable and efficient tool for accurately detecting changes in land use and land cover across large areas. This data may help to explain local changes observed for different LULC types. The study used eight Landsat pictures from over 36 years, taken in 1985, 1990, 1995, 2000, 2005, 2010, 2015, and 2021, to make land use maps using maximum likelihood classification methods. These maps included a signature file for the western Nile delta region. According to the different land cover types existing in the study area, the signature file was created by selecting four classes. The selected classes of land cover were water, agricultural, urban, and bare land. The results show that agricultural classes increased by 64% from the year 1985 to 2021; after being about 1.9% in 1985, they now occupy 66% in 2021. However, the bare land had decreased due to the increase of urban and agricultural lands. The results of SCS indicated that the sequester carbon in soil ranged mostly from 600 to 1800 g/m^2. This estimation is highly valuable for strategizing sustainable plans in agriculture, as well as for the effective management of water resources and future projects related to agricultural, urban development, and water management.

References

[1] H. El-Ramady, M. Abowaly, F. Elbehiry, A. E. Omara, T. Elsakhawy, S. Mohamed, A. Belal, H. Elbasiouny, Z. Abdalla, Stressful Environments and Sustainable Soil Management: A Case Study of Kafr El-Sheikh, Egypt, Environ. Biodivers. Soil Secur 3 (2019) 41–50.

[2] E. Elimy, A. Hassan, M. Omar, P. Riad, Land Use /Land Cover Change Detection Analysis for Eastern Nile Delta Fringes, Egypt, Environ. Earth Sci 10 (2020) 65–78.

[3] A. A. Barati, M. Zhoolideh, H. Azadi, J. H. Lee, J. Scheffran, Interactions of land-use cover and climate change at global level: How to mitigate the environmental risks and warming effects, Ecol. Indic 146 (2023) 109829–109829.

[4] S. Beshir, A. Moges, M. Dananto, Trend analysis, past dynamics and future prediction of land use and land cover change in upper Wabe-Shebele river basin, Heliyon 9 (2023).

[5] H. Feng, P. Kang, Z. Deng, W. Zhao, M. Hua, X. Zhu, Z. Wang, The impact of climate change and human activities to vegetation carbon sequestration variation in Sichuan and Chongqing, Environ. Res 238 (2023) 117138–117138.

[6] S. Gutierrez, D. Grados, A. B. Møller, L. D. C. Gomes, A. M. Beucher, F. Giannini-Kurina, L. W. D. Jonge, M. H. Greve, Unleashing the sequestration potential of soil organic carbon under climate and land use change scenarios in Danish agroecosystems, Sci. Total Environ 905 (2023) 166921–166921.

[7] R, Soil carbon sequestration to mitigate climate change, Geoderma 123 (2004) 1–22.

[8] D. A. N. Ussiri, R. [link].
URL https://doi.org/10.1007/978-3-319-53845-7

[9] M. E. Abd-Elmaboud (2016).

[10] C. Xu, Q. Zhang, Q. Yu, J. Wang, F. Wang, S. Qiu, M. Ai, J. Zhao, Ecol. Indic 151 (2023) 110345–110345.

[11] S. S. Rwanga, J. M. Ndambuki, Accuracy Assessment of Land Use/Land Cover Classification Using Remote Sensing and GIS, Int. J. Geosci 08 (2017) 611–611.

[12] N. Bakr, I. Morsy, H. A. Yehia, Spatio-temporal land use/cover detection and prediction in Mediterranean region: A case study in Idku ecosystem, Appl. Soc. Environ 25 (2022) 100673–100673.

[13] B. K. Arsiso, G. M. Tsidu, N. T. Abegaz, Impact of land use and land cover change on land surface temperature over Lake Tana Basin, J. Afr. Earth Sci 207 (2023) 105047–105047.

[14] Y. Hu, A. Raza, N. R. Syed, S. Acharki, R. L. Ray, S. Hussain, H. Dehghanisanij, M. Zubair, A. Elbeltagi, Land Use/Land Cover Change Detection and NDVI Estimation in Pakistan's Southern Punjab Province, Sustainability 15 (2023) 3572–3572.

[15] T. Lillesand, R. W. Kiefer, J. Chipman (2015).

[16] K. Abutaleb, S. W. Newete, E. Adam, F. Nsanganwimana, M. J. Byrne, J. A. Mukarugwiro, Mapping spatio-temporal variations in water hyacinth (Eichhornia crassipes) coverage on Rwandan water bodies using multispectral imageries, Int. J. Environ. Sci. Technol 18 (2021) 275–286.

[17] V. Adjei, M. Antwi, Land use change detection using the intensity analysis at the Bosomtwe District, Smart Agric. Technol 5 (2023) 100290–100290.

[18] P. Devkota, S. Dhakal, S. Shrestha, U. B. Shrestha, Land use land cover changes in the major cities of Nepal from, Environ. Sustain. Indic 17 (1990) 100227–100227.

[19] J. Rogan, D. Chen, Remote sensing technology for mapping and monitoring land-cover and land-use change, Prog. Plan. - PROG PLANN 61 (2004) 66–73.

[20] N. Bakr, M. H. Bahnassy, Land use/land cover and vegetation status, Soils Egypt (2019) 51–67.

[21] M. W. A. Halmy, P. E. Gessler, J. A. Hicke, B. B. Salem, Land use/land cover change detection and prediction in the north-western coastal desert of Egypt using Markov-CA, Appl. Geogr 63 (2015) 101–112.

[22] A. Singh, Review Article Digital change detection techniques using remotely-sensed data, Int. J. Remote Sens 10 (1989) 989–1003.

[23] N. Bakr, A. A. Al-Janabi, A. S. Suliman, E. M. Elzahaby, Land Cover Change Detection and Land Evaluation of Burg El Arab Region, North West Coast, Egypt, 2015.

[24] A. L, P. J, A. J, Automatic forest change detection through a bi-annual time series of satellite imagery: Toward production of an integrated land cover map, Int. J. Appl. Earth Obs. Geoinformation 118 (2023) 103289–103289.

[25] P. N. Dixit, G. M. Richter, K. Coleman, A. L. Collins, Bioenergy crop production and carbon sequestration potential under changing climate and land use: A case study in the upper River Taw catchment in southwest England, Sci. Total Environ 900 (2023) 166390–166390.

[26] T. B. Feitosa, M. M. Fernandes, C. A. G. Santos, R. M. Silva, J. R. Garcia, R. N. D. A. Filho, M. R. Fernandes, E. R. D. Cunha, Assessing economic and ecological impacts of carbon stock and land use changes in Brazil's Amazon Forest: A 2050 projection, Sustain. Prod. Consum 41 (2023) 64–74.

[27] R. Sharma, S. K. Chauhan, A. M. Tripathi, Carbon sequestration potential in agroforestry system in India: an analysis for carbon project, Agrofor. Syst 90 (2016) 631–644.

[28] S. R. Conrad, I. R. Santos, S. A. White, C. J. Holloway, D. R. Brown, P. D. Wadnerkar, R. E. Correa, R. L. Woodrow, C. J. Sanders, Land use change increases contaminant sequestration in blue carbon sediments, Sci. Total Environ 873 (2023) 162175–162175.

[29] F. Zhang, N. Xu, C. Wang, F. Wu, X. Chu, Phys. Chem. Earth Parts ABC 120 (2020) 102948–102948.

[30] M. Abdipour, S. M. Hoseini, H. Kaboli, M. K. K. Golafshani, Effect of Land Use Change on Carbon Sequestration: A Case Study in Shahmirzad Walnut Orchad, Res. J. Soil Biol 7 (2015) 1–12.

[31] O. R. El-Kawy, J. K. Rød, H. A. Ismail, A. S. Suliman, Land use and land cover change detection in the western Nile

delta of Egypt using remote sensing data, Appl. Geogr 31 (2011) 483–494.
[32] Y. Ban, O. Yousif, Change Detection Techniques: A Review, Methods Appl (2016) 19–43.
[33] E. G. Jobbágy, R. B. Jackson, The Vertical Distribution of Soil Organic Carbon and Its Relation to Climate and Vegetation, Ecol. Appl 10 (2000) 423–436.
[34] M. Abu-Hashim, M. Elsayed, A. E. Belal, Effect of land-use changes and site variables on surface soil organic carbon pool at Mediterranean Region, J. Afr. Earth Sci 114 (2016) 78–84.
[35] R, World soils and greenhouse effect : An overview, Soils Glob, Change (1995) 1–7.
[36] R, Soil carbon sequestration to mitigate climate change, Geoderma 123 (2004) 1–22.
[37] L. Pan, C. He, S. Jiang, Factors influencing degree of substitution of phosphate monoester of sweet potato starch, Nongye Gongcheng XuebaoTransactions Chin. Soc. Agric. Eng 18 (2002) 100–100.
[38] A. M. Abdulaziz, J. José, M. Hurtado, R. Al-Douri, Application of multitemporal Landsat data to monitor land cover changes in the Eastern Nile Delta region, Int. J. Remote Sens 30 (2009) 2977–2996.
[39] I. Esam, F. Abdalla, N. Erich, Land Use and Land Cover Changes of West Tahta Region, Sohag Governorate, Upper Egypt, J. Geogr. Inf. Syst 4 (2012) 483–493.
[40] R. Alvarez, C. R. Alvarez, Soil organic matter pools and their associations with carbon mineralization kinetics, Soil Sci. Soc. Am. J 64 (2000) 184–189.
[41] Z. X. Tan, R. Lal, N. E. Smeck, F. G. Calhoun, R. M. Gehring, B. Parkinson, Identifying associations among soil and site variables using canonical correlation analysis, Soil Sci 168 (2003) 376–382.
[42] D. Chen, D. A. Stow, P. Gong, Examining the effect of spatial resolution and texture window size on classification accuracy: An urban environment case, Int. J. Remote Sens 25 (2004) 2177–2192.
[43] E. G. Jobbágy, R. B. Jackson, The vertical distribution of soil organic carbon and its relation to climate and vegetation, Ecol. Appl 10 (2000) 423–436.
[44] M. Abu-Hashim, E. Mohamed, A. E. Belal, Identification of potential soil water retention using hydric numerical model at arid regions by land-use changes, Int. Soil Water Conserv. Res 3 (2015) 305–315.
[45] P. J. A. Howard, P. J. Loveland, R. I. Bradley, F. T. Dry, D. M. Howard, D. C. Howard (1995). [link].
URL https://doi.org/10.1111/j.1475-2743.1995.tb00488.x
[46] Ipcc, ipcc special report on carbon dioxide capture and storage, Cambridge University Press, 2005.
[47]
[48] U. Website. [link].
URL https://www.earthexplorer.usgs.gov